J Fluoresc (2010) 20:703–712
DOI 10.1007/s10895-010-0611-7

ORIGINAL PAPER

Synthesis, Spectroscopy and Photochemistry of Novel Branched Fluorescent Nitro-Stilbene Derivatives with Benzopheonone Groups

Fang Gao · Jian Liu · Huayong Peng · Nvdan Hu · Hongru Li · Shengtao Zhang

Received: 8 November 2009 / Accepted: 7 February 2010 / Published online: 23 February 2010

Abstract In this article, we presented novel nitro-stilbene derivatives with one or two benzophenone groups as photo-initiators via multi-steps synthesis. The ultraviolet/visible spectroscopy and the emission spectroscopy of the compounds were determined in various solvents. The results showed that the ultraviolet/visible absorption spectroscopy of the derivatives with benzophenone moiety displayed overlap effects of nitro-stilbene and benzophenone parts. In non-polar solvents, the derivatives exhibited strong emission, while they displayed weak emission in modest and strong polar solvents. Dyes-linked benzopheonone groups displayed stronger fluorescence emission than simple chromophore parent molecules. Visible-light photoinitiating effects of the derivatives were investigated extensively. Methyl methacrylate could be photoinitiated efficiently by the derivatives with benzophenone moieties at very low concentration, even at 1×10^{-5} mol/L. While the photopolymerization efficiency of styrene initiated by the derivatives was lower than that of methyl methacrylate. Our results showed that the dye-linked photo-initators had more efficient photoinitiating than the simple mixture of dye and photoinitator. Furthermore, the derivative with two benzophenone groups displayed more excellent phototiniatiating effects than the derivative with one benzophenone group. Thermodynamics driving for the occurrence of visible-light photoinduced intramolecular electron transfer from chromophore part to benzophenone part was evaluated. Benzopinacol moiety produced in photoreaction was confirmed by nuclear magnetic resonant spectroscopy. Thermal stability of the derivatives was analyzed.

F. Gao (✉) · J. Liu · H. Peng · N. Hu · H. Li · S. Zhang
College of Chemistry and Chemical Engineering,
Chongqing University,
Chongqing 400044, China
e-mail: fanggao1971@gmail.com

Keywords Synthesis · Ultraviolet/visible absorption spectroscopy · Fluorescence spectroscopy · Photochemistry · Nitro-stilbene · Benzophenone

Introduction

In recent years, with the development of long-wavelength laser technology, visible-light photopolymerization has received considerable attention due to superior advantages such as easy fabrication of various micro-devices, rapid dental photocuring, negligible damage to biological tissue, less costs and so on [1–8]. Extensive efforts using intermolecular dye-sensitization for visible-light photopolymerization have been devoted to achieve high efficient visible-light photopolymerization, which could guarantee use of lower sample concentrations in application [9–12]. For instance, iodonium salts and sulfonium salts, which are two sorts of typical ultraviolet photoinitators, were sensitized efficiently by visible light dyes including squaraine dyes and ketone dyes to produce free radicals for photopolymerization of vinyl ethers monomer and epoxides under visible light irradiation [13, 14]. It was demonstrated that dye molecules played the role of absorption of visible light, and photoinduced intermolecular electron transfer between visible light dyes and ultraviolet photoinitators occurred. Consequently, the photosensitive initiating efficiency of the dye-sensitization system was dependent on the rate of photoinduced electron transfer, which played significant role on photochemistry and photophysics such as fluorescence sensors and fluorescence switches. While as compared with intramolecular electron transfer, relative slow intermolecular photochemical rate limited further enhancement of visible-light photochemistry efficiency. Accordingly, the development of dye-linked photoinitators

became a research focus [15, 16]. This provided great possibility on the realization of highly efficient visible-light photopolymerization through photoinduced intramolecular electron transfer. However, the construction of such novel photofunctional compounds with required and ideal photochemical and photophysical properties is always challenge for chemists. For instance, one of shortcomings is that coupling an ultraviolet photoinitator with a known chromophore always leads to the fluorescence attenuation of chromophore part due to the interaction of chromophore part and functional molecule [17, 18].

Of particular interests for us is if we could build some dye-linked photosensitive compounds, which not only exhibit great visible-light photoinitiating efficiency, but have excellent photoluminescent nature. Herein, we proposed a new chemical strategy, which employed branched dye-linked benzophenone as long-wavelength photoinitiators. It is well-known that benzophenone is typical ultraviolet photoinitiator [19]. If more benzophenone parts are packed in the same dye molecule, they could provide much more efficient visible-light photopolymerization. Furthermore, because benzophenone has rigid structure, the fluorescence emission of chromophore part could be enhanced as coupling with benzophenone part via covalent bonds. This paper is part of our endeavor on the achievement of the above goal, which concentrated on particularly the building branched dye-linked photoinitiators. The spectroscopy, the photochemistry as well as thermal stabilities were exclusively investigated.

Experimental

Materials

The organic solvents were purchased from Chongqing Oriental Chemical Corporation and further dried using standard laboratory techniques according to published method [20]. Other reagents were obtained from Aldrich unless otherwise specified. **C2**, **C3**, **C4**, **C5** and **C6** (Fig. 1) were synthesized in our laboratory (Fig. 2).

Instruments

The UV/visible absorption spectra (1×10^{-5} mol/L) were recorded with a Cintra spectrophotometer. The emission spectra (1×10^{-5} mol/L) were determined with Shimadzu RF-531PC spectrofluorophotonmeter, which was fitted with a 150 W xenon lamp operated as a continuous wave source, slits selectable in six steps to produce spectral bandwidths of 1.5, 3, 5, 10, 15 and 20 nm. Rodamin 6G in ethanol (Φ=0.94, 1×10^{-6}–1×10^{-5} mol/L [21, 22]) was used as reference to determine the fluorescence quantum yields of the compounds herein. To avoid self-quenching of fluorescence emission, the low concentration of the compounds (1×10^{-6} mol/L) was prepared for the survey of fluorescence quantum yields. The melting point was determined using a Sichuan University 2X-1 melting point apparatus and was uncorrected. Nuclear Magnetic Resonance (NMR) was done at room temperature with a Bruker 500 MHz apparatus with tetramethylsilane (TMS) as internal standard and $CDCl_3$ as solvent. Element analysis was detected by CE440 elemental analysis meter from Exeter Analytical Inc.

The fluorescence quantum yields of the compounds in solvents with different polarities were measured based on the following equation.

$$\Phi_f = \Phi_f^0 \frac{n_0^2 A^0 \int I_f(\lambda_f)d\lambda_f}{n^2 A \int I_f^0(\lambda_f)d\lambda_f}$$

wherein n_0 and n were the refractive indices of the solvents, A^0 and A were the absorption of the reference and the sample at excited wavelength respectively, Φ_f and Φ_f^0 were the quantum yields, and the integrals denoted the area of the fluorescence bands for the reference and the sample respectively.

Visible-light photochemistry

Nitro-stilbene dyes (photoinitiators), ethanolamine (as coinitiator) and monomer were dissolved in ethyl acetate in dark. Photopolymerization was performed in a 10 cm pyrex tube as irradiated by a 1KW tungsten-iodine lamp as light source at 10 cm distance. The photochemical reaction was carried out at room temperature via condenser water and strong fan to remove thermopolymerization. The wavelength below 380 nm was cut off by the filter in order to remove ultraviolet light photopolymerization. Photopolymer was precipitated in cold methanol, and dried by vacuum, and weighted to calculate visible-light photopolymerization yields.

Thermal analysis

The differential thermal analysis (DTA) and thermograving (TGA) were conducted under nitrogen flow in Shimadzu DTG-60H equipment at heating rate 10°C min^{-1}.

Synthesis

Synthesis route was presented in Fig. 2.

(1) ***C2**: 4-bromomethyl benzophenone*

The compound was synthesized according to a well-known method with modified procedure [23].

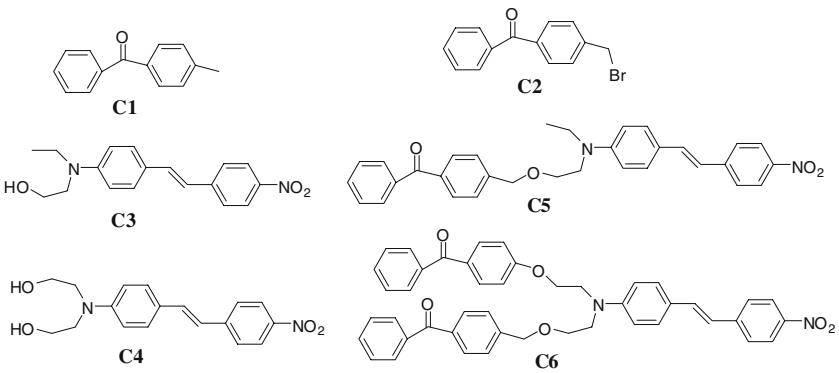

Fig. 1 The chemical structures of **C1**, **C2**, **C3**, **C4**, **C5** and **C6** studied in this paper

(2) ***C3****: p-N-ethyl-N-hydroxylethylamino-p′-nitro-stilbene*

p-N-Ethyl-N-hydroxylethylamino-benzaldehyde was prepared according to a reported method with Vilsmeier-Haack formylation via protection and deprotection procedure [24]. **C3** was prepared according to a similar method with modified procedure [25]. 2 g p-Nitro-phenylacetic acid (11 mmol) and 1.54 g p-N-ethyl-N-hydroxylethyl-amino-benzaldehyde (8 mmol) were mixed fully, and 1.04 g (12 mmol) piperidine was added into the mixture. The resulting mixture was heated at 100°C for 2 h, then at 120°C for 1 h till a black solid was formed. The product 1.5 g (yield: 76%) was obtained as a brown solid after twice recrystallization from ethanol. ^{1}H-NMR, 1.125–1.154 (t, J= 7.25 Hz, 3H, –CH_3), 3.419–3.462 (m, 2H, –CH_2–), 3.469–3.492 (t, J=5.75 Hz, 2H, –CH_2–), 3.755–3.778 (t, J= 5.75 Hz, 2H, –CH_2–), 4.248–4.270 (t, J=5.5 Hz, 1H, H–O), 6.692 (s, 2H, Ar–H), 6.842–6.875 (d, J=16.5 Hz, 1H, –CH=CH–), 7.101–7.134 (d, J=16.5 Hz, 1H, –CH=CH–), 7.368 (s, 2H, Ar–H), 7.479–7.496 (d, J=8.5 Hz, 2H, Ar–H), 8.091–8.108 (d, J=8.5 Hz, 2H, Ar–H). Melting point (147–148°C), Anal. Calcd for $C_{18}H_{20}N_2O_3$, C, 69.21, H, 6.45, N, 8.97, O, 15.37. Found: C, 68.83, H, 6.53, N, 8.89.

(3) ***C4****: p-(N, N-dihydroxyethyl)amino-p′-nitro-stilbene*

p-(N,N-Dihydroxyethyl)amino-benzaldehyde was prepared according to the reported method [24]. **C4** was synthesized according to a similar method with modified procedure [25]. 2.68 g (14.8 mmol) *p*-Nitro-phenylacetic acid and 2.46 g (11.8 mmol) *p*-(N,N-dihydroxyethylamino)-*p′*-nitro-benzaldehyde were mixed fully and 1.5 g piperdine (17.6 mmol) was added into the mixture. The resultant mixture was heated at 100°C for 2 h, then at 120°C for 1 h till a black solid was formed. 2.5 g (yield: 71.4 %) **C5** was obtained as a brown solid after twice crystallization from ethanol. ^{1}H-NMR δ: 3.450–3.475 (t, J=6.25 Hz, 4H, –O–CH_2–), 3.537–3.562 (t, J= 6.25 Hz, 4H, –N–CH_2–), 4.795–4.817 (t, J=5.5 Hz, 2H, H–O), 6.713–6.730 (d, J=8.5 Hz, 2H, Ar–H), 7.060–7.093

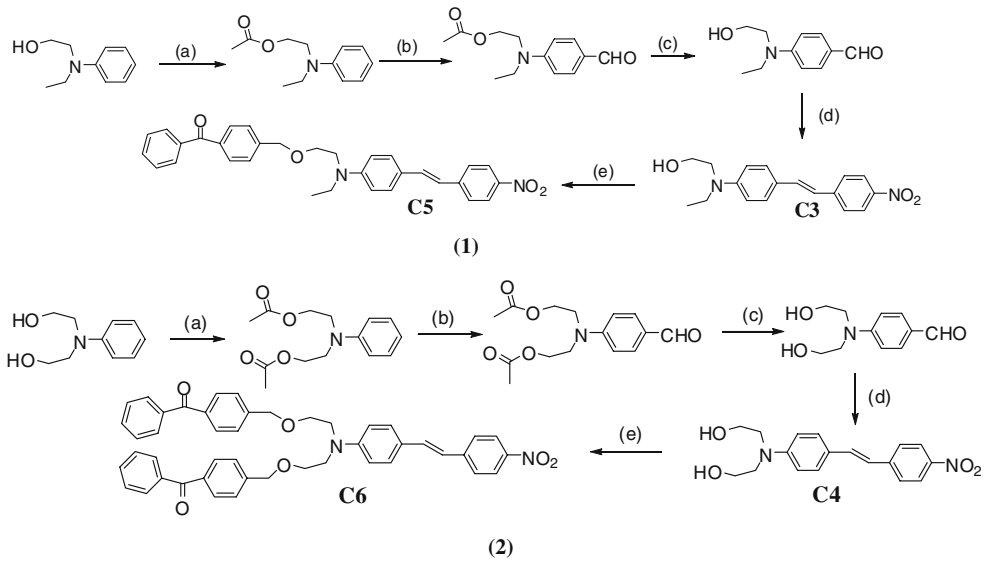

Fig. 2 The synthesis route of **C5** and **C6**

(1), **(2) :** (a) pyridine, acetic anhydride, (b) DMF/$POCl_3$, (c) NaOH/CH_3CH_2OH, (d) piperidine, phenylacetic acid, (e) 4-bromomethylbenzophenone, NaH/THF

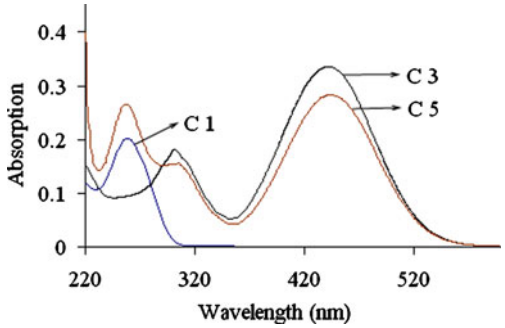

Fig. 3 Typical UV/visible spectroscopy of **C1**, **C3** and **C5** in acetonitrile ($c=1\times10^{-5}$ mol/L)

(d, J=16.5 Hz,1H, –CH=CH–), 7.377–7.410 (d, J=16.5 Hz,1H, –CH=CH–), 7.457–7.474 (d, J=8.5 Hz, 2H, Ar–H), 7.737–7.754 (d, J=8.5 Hz, 2H, Ar–H), 8.160–8.177 (d, J=8.5 Hz, 2H, Ar–H). Melting point (168–1169°C), Anal. Calcd for $C_{18}H_{20}N_2O_4$, C, 65.84, H, 6.14, N, 8.53, O, 19.49. Found: C, 65.69, H, 6.21, N, 8.67.

(4) *C5, 4-[N-ethyl-N-(2-(p-benzoyl-phenylmethoxyl) ethyl]-4'-nitro-stilbene*

Crude sodium hyride was washed by dry cyclohexane twice to remove mineral oil. **C2** 2.75 g (10 mmol) and **C3** (1.56 g, 5 mmol) were dissolved in NaH/50 ml dry THF, the mixture was stirred at room temperature under argon for 24 h. The solid was got rid of solution by filtration and THF was removed fully by evaporation. The resulting mixture was dissolved in chloroform and washed by water for three times. The organic layer was dried with anhydrous sodium sulfate and then concentrated. The product was purified by column chromatography. Further purification was carried out with twice recrystallization from benzene to yield 0.8 g (1.6 mmol) deep red solid of **C5** (yield 31.5%). ^{1}H-NMR δ: 1.150 (s, 3H, $–CH_3$), 3.438 (s, 2H, $–N–CH_2–$), 3.263 (s, 2H, $–N–CH_2–$), 3.705 (s, 2H, $–O–CH_2–$), 4.517 (s, 2H, $–O–CH_2–Ar$), 6.865–6.896 (d, J=15.5 Hz, 1H, –CH=CH–), 7.104–7.136 (d, J=14.0 Hz, 1H, –CH=CH–), 7.313 (s, 2H, Ar–H), 7.381–7.411 (t, J=7.5 Hz, 4H, Ar–H), 7.483–7.520 (m, 4H, Ar–H), 7.697–7.711 (t, J=3.5 Hz, 5H, Ar–H), 8.158–8.176 (d, J=9.0 Hz, 2H, Ar–H). ^{13}C-NMR: 13.124, 45.251, 69.731, 71.531, 72.409, 124.162, 126.564, 126.905, 127.249, 127.951, 128.311, 130.038, 130.285, 132.470, 132.765, 135.969, 136.908, 137.564, 140.600, 142.992, 143.709, 146.823, 196.389. Melting point (88–90°C), Anal. Calcd for $C_{32}H_{30}N_2O_4$, C,75.87, H, 5.97, N, 5.53, O, 12.63. Found: C, 75.78, H, 6.13, N, 5.45.

(5) *C6, 4-N, N-di[(2-(p-benzoyl-phenylmethoxyl)ethyl]-4'-nitro-stilbene*

The title compound was synthesized by a similar procedure as **C5**. Crude NaH was washed by dry cyclohexane twice to remove mineral oil. **C2** 5.5 g (20 mmol) and **C4** (1.64 g, 5 mmol) were dissolved in NaH/50 ml dry THF, the mixture was stirred at room temperature under argon for 20 h. The solid was got rid of solution by filtration and THF was removed fully by evaporation. The resulting mixture was dissolved in chloroform and washed by water for three times. The organic layer was dried with anhydrous sodium sulfate and then concentrated. The product was purified by column chromatography. Further purification was carried out with twice recrystallization from benzene to yield 1.22 g (1.7 mmol) deep red solid of **C6** (yield34.2%). ^{1}H-NMR δ: 3.736 (s, 8H, $–CH_2–$), 4.590 (s, 4H, $–O–CH_2–Ar$), 6.747–6.763 (d, J=8.0 Hz, 2H, Ar–H), 6.893–6.926 (d, J=16.5 Hz, 1H, –CH=CH–), 7.161–7.194 (d, J=16.5 Hz, 1H, –CH=CH–), 7.400–7.416 (d, J=8.0 Hz, 6H, Ar–H), 7.448 (s, 1H, Ar–H), 7.463 (s, 2H, Ar–H), 7.479 (s, 1H, Ar–H), 7.533 (s, 1H Ar–H), 7.551–7.559 (m, 2H, Ar–H),7.572 (s, 1H, Ar–H), 7.765–7.780 (t, J=3.5 Hz, 8H, Ar–H), 8.158–8.176 (d, J=9.0 Hz, 2H, Ar–H). ^{13}C-NMR: 51.947, 67.880, 77.348, 111.834, 121.634, 124.143, 125.334, 126.222, 127.075, 128.319, 128.599, 130.009, 130.271, 132.462, 133.222, 136.900, 137.587, 142.850, 144.772, 145.999, 196.304. Melting point (102–103°C), Anal. Calcd for $C_{46}H_{40}N_2O_6$, C, 77.08, H, 5.62, N, 3.91, O, 13.39. Found: C, 76.92, H, 5.71, N, 3.83.

Table 1 The absorption spectral data of **C3**, **C4**, **C5** and **C6** in various solvents

Solvents	λmax (nm)				$\varepsilon:\left(1\times10^5\right)\mathrm{L/mol\cdot cm}$			
	C3	**C4**	**C5**	**C6**	**C3**	**C4**	**C5**	**C6**
Cyclohexane	419	–	423	420	–	–	–	–
Benzene	436	431	436	431	0.2952	0.2875	0.2944	0.2832
Ethyl acetate	440	435	437	433	0.4614	0.4526	0.3607	0.3334
THF	444	443	442	436	0.3741	0.3555	0.3282	0.3113
CH_2Cl_2	443	443	446	440	0.3355	0.3058	0.2968	0.2738
CH_3CN	439	436	439	439	0.4078	0.3680	0.3529	0.3112

Results and discussion

Synthesis

4-Bromethyl-benzophenone, which was prepared from bromide reaction of 4-methyl-benzophenone and N-bromosuccinimide, played the role of the introduction of benzophenone moiety to the nitro-stilbene backbone. Owing to the electron-withdrawing effect of nitro group of *p*-nitro-phenylacetiac acid and the electron-donating of N, N-diethylamino group of benzaldehyde derivatives, **C3** and **C4** were produced by the condensation in the presence of weak base piperidine, which was carried out at high temperature to ensure full decarboxylation. **C5** or **C6** was prepared by **C2** and **C3** or **C4** respectively for the formation of ether bond using sodium hydride as base in mild conditions, and an acceptable yield was obtained. The combination use of flash column chromatography and recrystallization was efficient on the purification of **C5** and **C6**.

UV/Visible absorption and fluorescence spectroscopy

Typical ultraviolet/visible spectroscopy of **C1**, **C3** and **C5** in acetonitrile was presented in Fig. 3. Clearly, the absorption in the short-wavelength region came from benzophenone part mainly. While, the absorption in the visible-light region could be assigned to nitro-stilbene part. The results suggested that the ultraviolet/visible absorption of dye-linked photoinitiators exhibited overlap effect of the chromophore and photoinitiator parts. This further demonstrated that benzophenone part was linked covalently with nitro-stilbene part.

The ultraviolet/visible spectral data of **C3**, **C4**, **C5** and **C6** were listed in Table 1. It showed that the absorption maxima of **C3** and **C4** displayed bathchromic shift with the

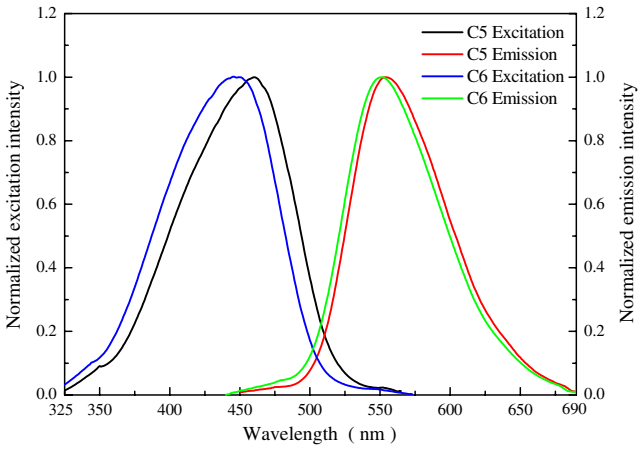

Fig. 4 Normalized excited and emission spectroscopy of **C5** and **C6** in benzene (Ex: 350 nm, c=5×10^{-6} mol/L)

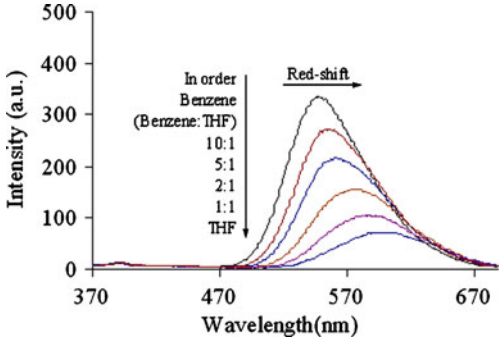

Fig. 5 The fluorescence change of **C6** with the increasing THF in THF/benzene binary solvents (Ex: 350 nm, Slit Width: Ex: 5 nm, Em: 3 nm, c=1×10^{-6} mol/L)

increasing of the solvent polarity (approximate 20 nm). This indicated that the long-wavelength absorption could be ascribed to strongly allowed (π, π*) transition with internal charge transfer nature [26]. Interesting, we observed that the optical density of maximal absorption wavelength of **C5** or **C6** was a little less than that of **C3** or **C4** respectively in various solvents. This implied that the benzophenone part had some influence on the molecular electron density distribution of chromophore part, and the electron transmission process of the compound was thus altered [27].

Mirror symmetry was observed for the excitation and temission spectroscopy of **C5** and **C6**, as shown in Fig. 4. **C3**, **C4**, **C5** and **C6** showed strong fluorescence emission in non-polar solvents such as in benzene. While, the photoluminescence became weak in polar solvents such as in THF and ethyl acetate. Typical fluorescence spectroscopy of **C6** in benzene/THF binary solvents was presented in Fig. 5. It clearly showed that with the increasing THF volume ratio in benzene/THF binary solvents, the fluorescent intensity of **C6** decreased, and the maximal fluorescence emission wavelength displayed red-shift gradually. This confirmed the existence of internal charge transfer at the excited state. Because diarylaminostilbene derivatives were typically characterized with twisted intramolecular

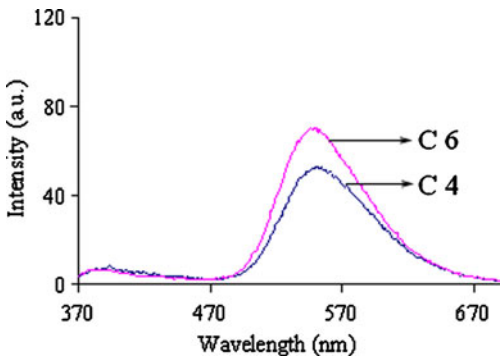

Fig. 6 Typical comparison of fluorescence spectroscopy of **C4** and **C6** in benzene (Ex: 350 nm, Slit Width: Ex: 3 nm, Em: 3 nm, c=1×10^{-6} mol/L)

Table 2 The maxima fluorescence emission wavelength and fluorescence quantum yields of **C3**, **C4**, **C5** and **C6** in various solvents

Solvents	$\lambda_{f,\ max}$ (nm)				Φ			
	C3	**C4**	**C5**	**C6**	**C3**	**C4**	**C5**	**C6**
Benzene	551	555	551	556	0.233	0.236	0.355	0.471
Ethyl Acetate	601	602	606	608	0.0330	0.0332	0.0533	0.0629
THF	602	601	607	609	0.0193	0.0198	0.0525	0.0710

charge transfer state in polar solvents [28], the derivatives exhibited strong fluorescence emission in apolar solvents and weak fluorescence emission in strong solvents.

C5 and **C6** exhibited stronger fluorescence emission than **C3** and **C4** in various solvents. Typical comparison of fluorescence spectroscopy of **C4** and **C6** in benzene was presented in Fig. 6. This showed that the fluorescence quantum yields of **C5** to **C6** were higher than those of **C3** and **C4** in various solvents, as shown in Table 2. The data indicated that the emission of the derivatives was increased by benzophenone parts. This could be understood from two aspects: (1) phenylmethyloxyl should have more stronger electron-donating effects that hydroxyl groups, thus the electron density distribution of chromophore of **C5** and **C6** was strengthened and their $\pi \rightarrow \pi^*$ electron transition could be enhanced, (2) the rigidity and stiffness of overall molecule were enhanced by benzophenone group. These might result in the enhancement of charge transfer, the limitation of cis-trans twist, the decreasing vibration of molecules, and the reduction of interaction of solute molecules, and accordingly the fluorescence emission of **C5** and **C6** became stronger [29].

Visible light photochemistry

We firstly investigated the possibility of visible-light photoinitiating of MMA with the system of benzophenone and triethanolamine. The results showed clearly that there was no production of PMMA, which was due to no absorption in the visible-light region for benzophenone and triethanolamine and thus no occurrence of photochemistry between them. We have carried out four photosensitive initiating systems for visible light polymerization in this study, which included **P1** (**C1**, **C3**, triethanolamine), **P2** (**C1**, **C4**, triethanolamine), **P3** (**C5**, triethanolamine), and **P4** (**C6**, triethanolamine).

The photopolymeric efficiency ratios of **P3** to **P1**, **P4** to **P2** were investigated. The ratio kept approximately constant with irradiation time at the fixed concentration of the photoinitiators. Typical results were presented as Fig. 7. The results suggested that **P1** and **P2** systems were able to photoinitiate the polymerization of monomer as they were irradiated by visible light, but the photopolymerization yields were lower than those of **P3** and **P4** respectively. The ratio was approximately 1.3 to 1.5 with irradiation time, indicating that the visible-light photosensitized initiating efficiency of **P3** and **P4** was much higher than that of **P1** and **P2** respectively. This demonstrated that free radicals produced from intramolecular photochemical reaction were much more than those from intermolecular photochemical reaction.

The plot of photopolymeric ratio of MMA of **P4** to **P3** with irradiation time was presented in Fig. 8. It showed that visible-light photoinitiating efficiency of **P4** was higher than that of **P3**, which suggested that two benzophenone parts induced a more efficient visible-light photopolymerization than one benzophenone part. The results suggested that branch effect played a significant role on the enhancement of visible-light photopolymerization efficien-

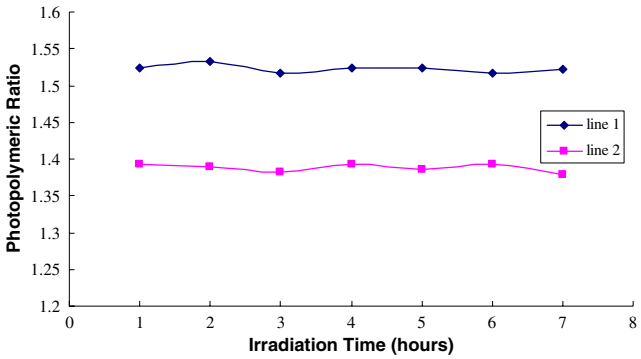

Fig. 7 The ratio of the photoinitiating polymerization yields of MMA with the irradiation time at the concentration 1×10^{-5} mol/L of the photoinitiators. Wherein MMA: 4.7 mol/L, triethanolamine: 2.65 mol/L, (**line 1**: **P4** to **P2**, **line 2**: **P3** to **P1**)

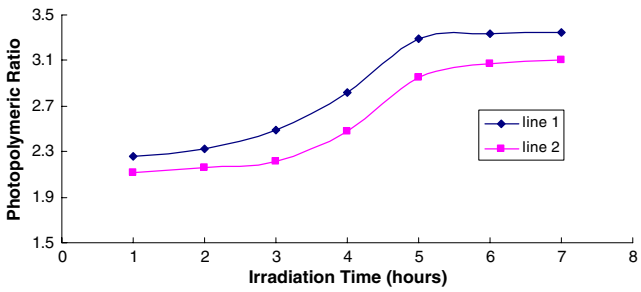

Fig. 8 The ratio of the photoinitiating polymerization yields of MMA to that of styrene with irradiation time at the concentration 1×10^{-5} mol/L of the photoinitiators. Where in: monomer: 4.7 mol/L, triethanolamine: 2.65 mol/L (**line 1**: MMA to styrene of **P4** system, **line 2**: MMA to styrene of **P3** system)

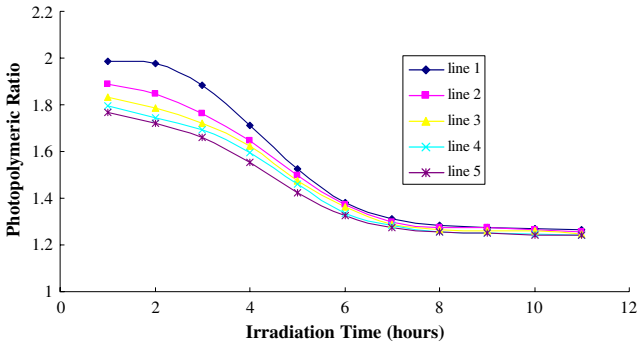

Fig. 9 The ratio of the photoinitiating polymerization yields of MMA (**P4** to **P3**) with irradiation time. Wherein: the concentration of compounds **5** and **6** for different lines: **line 1**: 1×10^{-5} mol/L, **line 2**: 2×10^{-5} mol/L, **line 3**: 3×10^{-5} mol/L, **line 4**: 4×10^{-5} mol/L, **line 5**: 5×10^{-5} mol/L, MMA: 4.7 mol/L triethanolamine: 2.65 mol/L

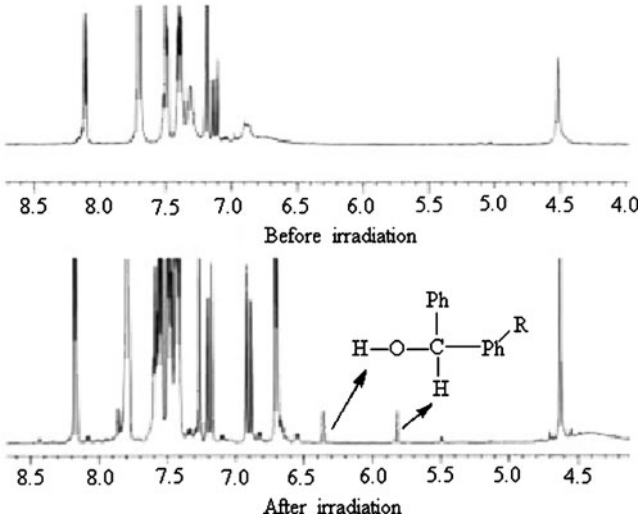

Fig. 10 The variation of ^{1}H-NMR of **C5**/triethanolamine system before and after irradiation

cy. With the increasing visible-light irradiation time, the radical coupling rate might increase due to more free radicals produced, and this could lead to decrease gradually the ratio of visible-light photoinitiating efficiency of **P4** to **P3** with irradiation time.

The visible-light photopolymerization of MMA and styrene photoinitiated by **P3** and **P4** was also studied. The plot of the photopolymeric ratio of MMA to that of styrene with the concentration of the photoinitiators was shown in Fig. 9. It showed clearly that the photopolymerization of MMA was more efficient than that of styrene, which was mostly due to the efficient quenching of excited triplet states of the photoinitiztors by styrene [30]. The ratio increased and reached approximately constant with irradiation time at the fixed concentration of the photoinitiators, which suggested that visible light photochemistry reaction kept relative stable with irradiation time. The effects of the coinitiators on the visible-light photopolymerization were also investigated. Triethanolamine displayed much more excellent photoinitiating effects than diethanolamine, monoethanolamine and triethylamine.

The value of free energy change ΔG for the electron transfer reaction between nitro-stilbenzene dyes and benzophenone was estimated according to the Rohm–Weller equation [31] and the results were listed in Table 3. Large negative ΔG suggested that photoinduced electron transfer between nitro-stilbenzene and benzophenone was allowed on thermodynamics. Accordingly, these compounds might undergo rapid visible light photochemistry during irradiation.

Photoinitiating mechanism of benzophenone/triethanolamine system was investigated well. Initiating free radicals for photopolymerization were formed via intermolecular hydrogen transfer from triethanolamine to benzophenone in the exciplex, which was formed through the triplet state of benzopheone [33, 34]. In the present study, the exciplex between photoiniator and triethanolamine could be formed at the excited state of photoinitator via intermolecular electron transfer as **C5** or **C6** was excited by the visible light. As discussed, the fluorescence quantum yields of **C5** and **C6** were higher than those of **C3** and **C4** respectively. Furthermore, visible light photopolymerization efficiency of styrene was bad. Thus, we assumed that photoinduced intramolecular electron transfer could occur through the

Table 3 The estimated values of free energy change ΔG of electron transfer between nitro-stilben dyes and benzopheone

$E^{ox}_{(D/D+)}$	$\Delta E_{0,0}{}^{(*)}$	ΔG
C3 0.512 ev	2.03 ev	−235.6 KJ/mol
C4 0.716 ev	2.01 ev	−214.0 KJ/mol

$E^{red}_{(A/A^-)}$ for benzopheone 0.925 ev [32]; estimation from the fluorescence emission*

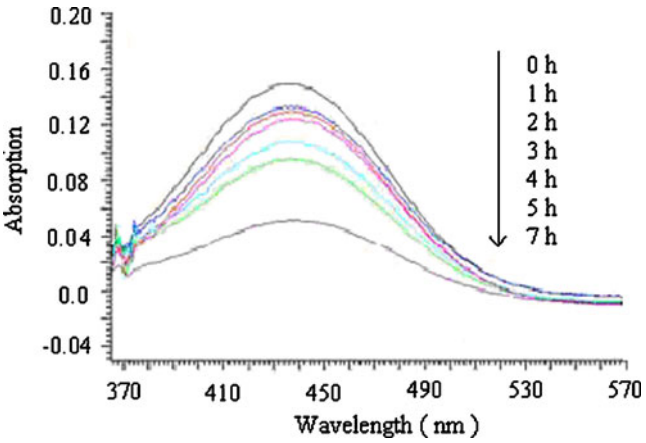

Fig. 11 The variation of the maximum absorption spectroscopy of **P3** system with visible-light irradiation time. Wherein: MMA: 4.7 mol/L, triethanolamine: 2.65 mol/L, the concentrations of **C5**: 4.5×10^{-6} mol/L, solvent: ethyl acetate

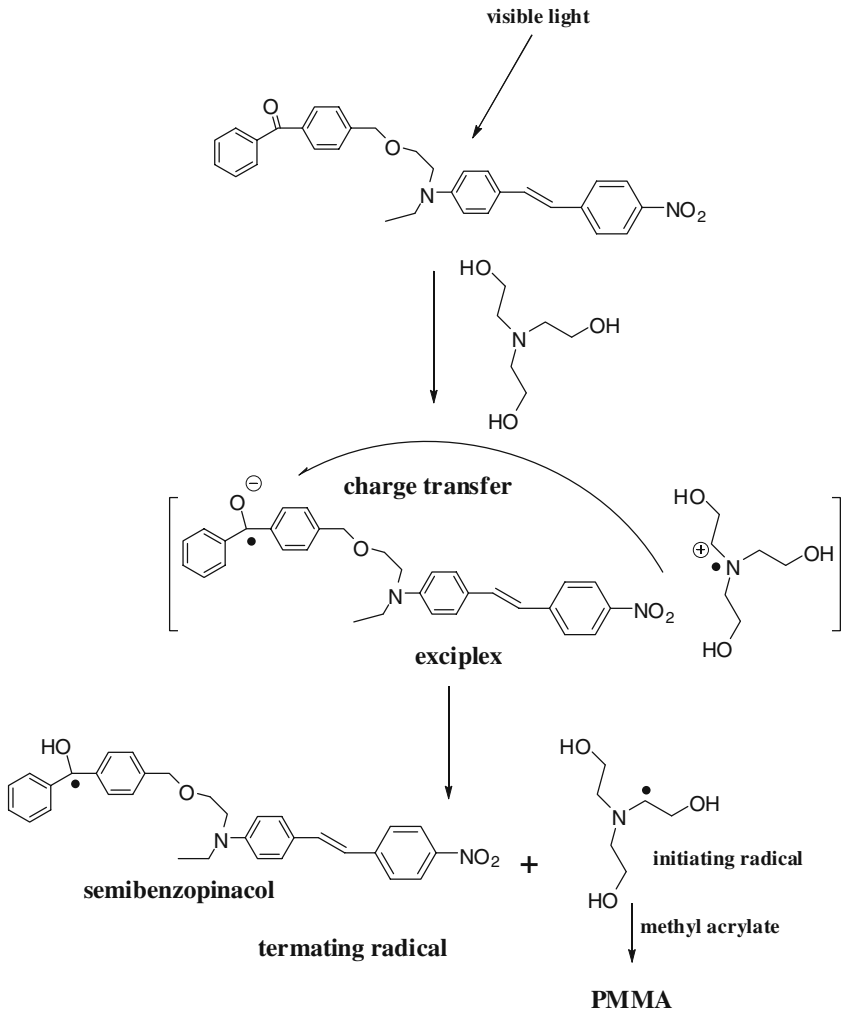

Fig. 12 A proposed photoinitiating polymerization processing for **C5**

excited triplet state of the chromophore part and benzophenone part.

Recently, semibenzopinacol moiety was successfully confirmed via the analysis of nuclear magnetic resonnan spectroscopy for ultraviolet light photopolymerization of benzophenone and triethanolamine photoinitiating system [35]. In this study, we performed the comparison of ^{1}H-NMR of the **C5**/triethanolamine system before and after irradiation to confirm the production of benzopinacol moiety during visible light photochemical reaction. As shown in Fig. 10, two new nuclear magnetic resonant peaks were detected during irradiation, which could be assigned to benzopinacol moiety.

Photobleaching could be observed for these photoinitiating systems only if sufficient polymer was produced, suggesting that semibenzopinacol might be attached to polymer tail. A typical variation of UV/visible spectra of **C5**/triethanolamine system was shown in Fig. 11. Because the percent of chromophore moiety in the polymer line was remarkably low, the color of the chromophore moiety could not be observed. **P3** and **P4** systems displayed more rapid photobleaching than **P1** and **P2** systems, which demonstrated that they had more efficient visible-light photochemistry. According to experimental observation and the references [35, 36], a possible photoinitating mechanism was proposed as presented in Fig. 12.

Thermal analysis

Thermal property of the derivatives was analyzed by the measurement of differential thermal analysis (DTA) and thermograving (TGA) under a nitrogen atmosphere. The onset decomposition temperatures of **C3**, **C4**, **C5** and **C6** determined by TGA were 335.77, 322.51, 328.10 and 331.81°C respectively as presented in Fig. 12, which suggested that the substitution of benzopheonone part did not play negative effect on the thermal stability of the compounds. The derivatives could be regarded as robust molecules. The weight loss of **C3** (MW=312.26) was 31.629% at 335.77°C, which was close to the loss of N-ethyl-N-hydroethyl group (MW=88.13). Interestingly, the weight loss of **C4** (MW=328.36) was 21.306% at 322.51°C,

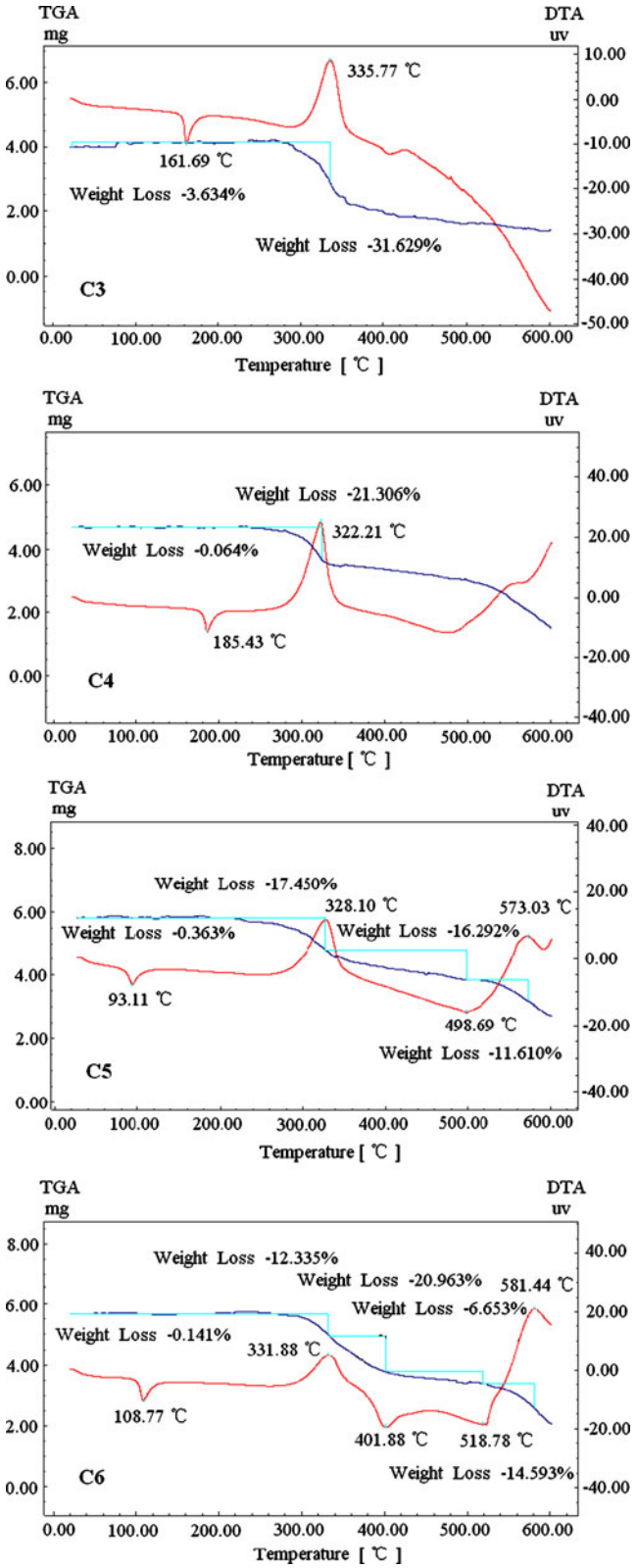

Fig. 13 DTA and TGA curves of the **C3**, **C4**, **C5** and **C6**

which was also close to the loss of two C–OH parts (MW= 64.08). The weight loss of **C5** (MW=522.59) was 17.450% at 328.10°C, which was close to the loss of phenyl ring (MW=78.11). Remarkably, **C6** (MW=702.79) displayed 12.355% weight loss at 331.81°C, which was perfectly same as that of **C5**, indicating the possible loss of phenyl ring as well. The analysis showed that: (1) the decomposition of the **C3**, **C4**, **C5** and **C6** did occur at high temperatures, and (2) thermal stabilities of dye-linked photoinitiators was not much influenced by the substitution of photoinitator parts (Fig. 13).

Conclusions

To summarize, novel fluorescent photoinitiators of dye-linked benzophenone via ether bond for visible-light photochemistry were synthesized and characterized. Remarkable solvatochromic effect was observed for the absorption and fluorescence spectroscopy of the derivatives. The occurrence of rapid visible light photoinduced intramolecular electron transfer of **C5** and **C6** could lead to much higher efficient long-wavelength photopolymerization, which was superior over those simple combinations (**P1** and **P2** systems). We have presented strong evidences that the branch effect was an efficient chemical strategy on the enhancement of visible-light photoinitating polymerization of acrylate ester. Novel photoinitators displayed almost the same thermal decomposed temperatures as the chromophore parent molecules, which demonstrated that the thermal stabilities of novel photoinitators were not reduced by the benzophenone groups.

Acknowledgements The authors appreciate financial support from National Natural Science Foundation of China (Nos. 20776165, 20702065, 20872184). We would thank the "Foundation of Chongqing Science and Technology Commission" (CSTC2008BA4020, CSTC2009BB4216). H. Li thanks "A Foundation for the Author of National Excellent Doctoral Dissertation of PR China (200735)" for financial support. This paper is partly sponsored by the Scientific Research Foundation for the Returned Overseas Chinese Scholars, State Education Ministry as well (Nos. 20071108-1, 20071108-5). The support from Innovative Talent Training Project, the Third State of "211 Project", Chongqing University (S-09103) is greatly appreciated.

References

1. Cumpston BH, Ananthavel SP, Barlow S, Dyer DL, Ehrlich JE, Erskine LL, Heikal AA, Kuebler SM, Lee IYS, Maughon DMC, Qin JQ, Röckel H, Rumi M, Wu XL, Marder SR, Perry JW (1999) Two-photon polymerization initiators for three-dimensional optical data storage and microfabrication. Nature 398:51–54
2. Gao F, Wang JC, Liu XJ, Yang L, Hu ND, Xie T, Li HR, Zhang ST (2009) Synthesis, spectroscopy and photochemistry of nitroazobenzene dyes bearing benzophenone parts. J Fluor 19(3):533–544

3. Hwang I, Son Y, Kim J, Jeon Y, Kim J, Lee C, Park J, Lee J (2008) Plasma-arc generated light inhibits proliferation and induces apoptosis of human gingival fibroblasts in a dose-dependent manner. Dental Mater 24(8):1036–1042
4. Zhu Y, Pavlos CM, Toscano JP, Dore TM (2006) 8-Bromo-7-hydroxyquinoline as a photoremovable protecting group for physiological use: Mechanism and scope. J Am Chem Soc 128 (13):4267–4276
5. Park SJ, Kyu T (2008) Photopolymerization-induced crystallization and phase separation in poly(ethylene oxide)/triacrylate blends. J Chem Phys 129(24):244901–244909
6. Kancharla VV, Chen SC (2002) Fabrication of biodegradable polymeric micro-devices Using laser micromachining. Biomed Microdevices 4(2):105–109
7. Ganster B, Fischer UK, Moszner N, Liska R (2008) New photocleavable structures. Diacylgermane-based photoinitiators for visible light curing. Macromolecules 41(7):2394–2400
8. Neumann MG, Schmitt CC, Maciel HM (2001) The effect of monomer aggregation in the photopolymerization of styrenesulfonate. J Phys Chem B 105(15):2939–2944
9. Natarajan LV, Brown DP, Wofford JM, Tondiglia VP, Sutherland RL, Lloyd PF, Bunning TJ (2006) Holographic polymer dispersed liquid crystal reflection gratings formed by visible light initiated thiol-ene photopolymerization. Polymer 47(12):4411–4420
10. Grotzinger C, Burget D, Jacques P, Fouassier JP (2001) A novel and efficient xanthenic dye-organometallic ion-pair complex for photoinitiating polymerization. J Appl Polym Sci 81(10):2368–2376
11. Ortuño M, Gallego S, García C, Neipp C, Pascual I (2003) Holographic characteristics of a 1-mm-thick photopolymer to be used in holographic memories. Appl Opt 42(35):7008–7012
12. Fouassier JP, Allonas X, Burget D (2003) Photopolymerization reactions under visible lights: principle, mechanisms and examples of applications. Prog Org Coat 47(1):16–36
13. Crivello JV, Sangermano M (2000) Visible and long-wavelength photoinitiated cationic polymerization. J Polym Sci, Part A Polym Chem 39(3):343–356
14. He Y, Zhou WH, Wu FP, Li MZ, Wang EJ (2004) Photoreaction and photopolymerization studies on squaraine dyes/iodonium salts combination. J Photochem Photobiol A 162(2–3):463–471
15. Kawamura K, Kato K (2004) Synthesis and evaluation as a visible-light polymerization photoinitiator of a new dye-linked bis(trichloromethyl)-1, 3, 5-triazine. Polym Adv Technol 15(6):324–328
16. Kawamura K, Aotani Y, Tomioka H (2003) Photoinduced intramolecular electron transfer between carbazole and bis(trichloromethyl)-s-triazine generating radicals. J Phys Chem B 107 (19):4579–4586
17. Gao F, Xie T, Cheng ZB, Hu ND, Yang L, Gong Y, Zhang ST, Li HR (2008) Synthesis, crystal, absorption and spectroscopy of nitrostilbene derivatives with benzophenones. J Fluoresc 18:787–799
18. Rusalov MV, Druzhinin SI, Uzhinov BM (2004) Intramolecular fluorescence quenching of crowned 7-aminocoumarins as potential fluorescent chemosensors. J Fluor 14(2):193–202
19. Jiang XS, Luo XW, Yin J (2005) Polymeric photoinitiators containing in-chain benzophenone and coinitiators amine: Effect of the structure of coinitiator amine on photopolymerization. J Photochem Photobiol A 174(2):165–170
20. Perrin D, Armarego W, Perrin D (1966) Purification of laboratory chemicals. Pergamon, New York
21. Maus M, Retigg W, Bonafoux D, Lapouyade R (1999) Photoinduced intramolecular charge transfer in a series of differently twisted donor-acceptor biphenyls as revealed by fluorescence. J Phys Chem A 103(18):3388–3401
22. Lukeman M, Veal D, Wan P, Ranjit V, Munasinghe N, Corrie JE (2004) Photogeneration of 1, 5-naphthoquinone methides via excited-state (formal) intramolecular proton transfer (ESIPT) and photodehydration of 1-naphthol derivatives in aqueous solution. Can J Chem 82(2):240–253
23. Itoh T, Hall HK (1990) 7-Chloro-7-phenyl-8, 8-dicyanoquinodimethane. a novel initiator for cationic polymerizations. Macromolecules 23 (22):4879–4881
24. Moon KJ, Shim HK, Lee KS, Zieda J, Prasad PN (1996) Synthesis, characterization, and second-order optical nonlinearity of a polyurethane structure functionalized with a hemicyanine dye. Macromolecules 29(3):861–867
25. Cavallini G, Massarani E (1959) Process for the preparation of 4-hydroxystilbene and its derivatives. US Patents No. 2878291
26. Zhang W, Mao W, Hu Y, Tian Z, Wang Z, Meng Q (2009) Phenothiazine-anthraquinone donor-acceptor molecules: synthesis, electronic properties and DFT-TDDFT computational study. J Phys Chem A 113(37):9997
27. Gao F, Hu N, Wang J, Yang L, Yang L, Li H, Zhang S (2009) Synthesis, two-photon properties and electrochemistry of A-B2 type nitro-stilbene dyes with benzophenone groups. Acta Phys-Chem Sin 25(7):1320
28. Zhang Q, Tour JM (1998) Alternating donor/acceptor repeat units in polythiophenes. Intramolecular charge transfer for reducing band gaps in fully substituted conjugated polymer. J Am Chem Soc 120(22):5355–5362
29. Tang BZ, Zhan X, Yu G, Lee PPS, Liu Y, Zhu D (2001) Efficient blue emission from siloles. J Mater Chem 11(12):2974–2978
30. Tasis DA, Siskos MG, Zarkadis AK (1998) 4-[Diphenyl(trimethylsilyl)methyl]benzophenone as initiator in the photopolymerization of methyl methacrylate and styrene. Macromol Chem Phys 199(9):1981–1988
31. Rehm D, Weller A (1970) Kinetics of fluorescence quenching by electron and H-atom transfer. Isr J Chem 8(2):259–271
32. Jockusch S, Timpe HJ, Schnabe IW, Turro NJ (1997) Photoinduced energy and electron transfer between ketone triplets and organic dyes. J Phys Chem A 101(4):440–445
33. Bhattacharyya K, Das PK (1986) Nanosecond transient processes in the triethylamine quenching of benzophenone triplets in aqueous alkaline media. Substituent effect, ketyl radical deprotonation and secondary photoreduction kinetics. J Phys Chem 90 (17):3987–3993
34. Gómez ML, Fasce DP, Williams RJJ, Balsells RE, Fatema MK, Nonami H (2008) Silsesquioxane functionalized with methacrylate and amine groups as a crosslinker/co-initiator for the synthesis of hydrogels by visible-light photopolymerization. Polymer 49 (17):3648–3653
35. Kong L, Deng J, Yang W (2006) Detailed 1D/2D NMR analyses of benzophenone-related reaction products from a photopolymerization system of vinyl acetate and benzophenone. Macromol Chem Phys 207(24):2311–2320
36. Kong L, Deng J, Xin L, Yang W (2008) Direct ether formation of semibenzopinacol moieties in a photopolymerization system featured constant intensity of absorbed light. Eur Poly J 44 (1):244–255